Si-Gly-CD-PdNPs as a hybrid heterogeneous catalyst for environmentally friendly continuous flow Sonogashira cross-coupling

ARTICLE

Si-Gly-CD-PdNPs as Hybrid Heterogeneous Catalyst for Environmentally Friendly Continuous Flow Sonogashira Cross-Coupling

Received 00th January 20xx,
Accepted 00th January 20xx

DOI: 10.1039/x0xx00000x

Francesco Ferlin,[a†] Daniele Sciosci,[a†] Federica Valentini,[a] Janet Menzio,[b] Giancarlo Cravotto,[b] Katia Martina,[b] Luigi Vaccaro *[a]

We have reported a waste-minimized protocol for the Sonogashira cross-coupling exploiting the safe use of CPME/water azeotropic mixture and the utilization of a heterogeneous hybrid palladium catalyst supported onto silica/β-cyclodextrin matrix in continuous flow. The use of the aq CPME azeotrope has proven to be crucial to enhance the catalyst performance including a very low metal leaching. In addition, we have also completed the flow protocol by setting a downstream in-line liquid/liquid separation that allows the continuous recovery and reuse of the CPME fraction leading to a consistent waste reduction. Finally, E-factor distribution and safety/hazard analysis have been performed highlighting the chemical and environmental efficiency of our protocol.

Introduction

Since its disclosure, the Sonogashira cross-coupling reaction[1] has been playing a pivotal role in organic synthesis. The formation of a new C–C bond between an acetylenic compound and an aromatic or aliphatic halide, in a fast and economical way, allows to the synthesis of several target compounds, i.e. active pharmaceutical ingredients as well as optoelectronic materials, with excellent yields.[2]

Nowadays, the demand for newly developed heterogeneous catalysts for cross-coupling[3] and more in general for metal catalysed C–C bond formation processes[4] is in continuous growth.[3] Indeed, a more sustainable approach to prepared the desired compounds with the possibility of easily remove and reuse metal-based catalytic systems is highly desirable.

Since '90s, hybrid catalytic systems, that consist of both inorganic and organic components, have been employed in a wide range of reactions.[5] The hybrid catalysts promise to combine heterogeneous and homogeneous advantages with the key possibility to tune the hybrid materials making them suitable for different catalytic pathways and conditions.[6]

The preparation of organic-inorganic hybrid systems can be approached in two ways. The first, and most used, consists in the grafting procedure which is accomplished by physical absorption. However, in this case, a non-homogeneous dispersion of the organic layer can be observed.[7] The secondo approach is based on the selective covalent grafting between the organic and the inorganic components and it represents a valid alternative to preserve the structure, morphology and porosity of the support material.[8]

The most explored supports are mesoporous materials,[9] polymers,[10] nanostructures[11] and metal organic frameworks (MOF).[12] While, the organic moiety can be a small molecule, or an oligomer and represent the anchored ligand. Among the latter, β-cyclodextrins (β-CDs) can be efficiently used as ligand/stabilizers for metal nanoparticles.[13] Due to their ability to host and stabilize metal ions and salts,[14] CDs have been widely exploited for the preparation hybrid organic-inorganic heterogeneous catalytic systems.[15]

Although, different heterogeneous catalysts and technologies have been developed to increase the efficiency of the Sonogashira reaction,[16] the use of continuous flow methodologies is relatively little explored.[17] When using a hybrid catalytic system it becomes of crucial utility the use of flow conditions where an improved stability and recoverability of the solid catalyst can be achieved.[18] In this regard, also the solvent selection plays a pivotal role in the efficiency of the whole strategy. Indeed, as demonstrated, it is possible to minimize metal leaching from a heterogeneous catalyst and expand its stability and use by a careful choice of the most appropriate solvent or solvent mixture.[19]

In this context, low-coordinating reaction media[20] or azeotropic mixtures can be the preferred choice. Moreover, the latter can also be in certain cases recyclable leading to a dramatic minimization of waste.[21]

[a] *Laboratory of Green S.O.C. – Dipartimento di Chimica, biologia e Biotecnologie, Università degli Studi di Perugia, Via Elce di Sotto 8, 06123 – Perugia, Italy. E-mail: luigi.vaccaro@unipg.it; http://greensoc.chm.unipg.it/ .*

[b] *Dipartimento di Scienza e Tecnologia del Farmaco, University of Turin, Via P. Giuria 9, 10125, Turin, Italy.*

† These authors contributed equally

Electronic Supplementary Information (ESI) available: [details of any supplementary information available should be included here]. See DOI: 10.1039/x0xx00000x

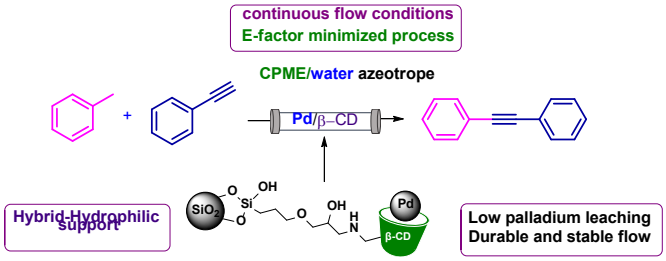

Scheme 1. Features of Si-Gly-CD-PdNPsβCD catalysed Sonogashira reaction in continuous flow.

In this contribution, after comparing a large number of potentially green and efficient reaction media, we focused our attention on aqueous cyclopentyl methyl ether (CPME) azeotrope. This medium proved to be crucial in influencing the catalytic performance of the hybrid Si-Gly-CD-PdNPsβ-CD heterogeneous catalyst. Indeed, taking advantages from the hydrophilic nature of β-CDligands, an easier access to the active catalytic sites occurs. Moreover, the presence of CPME and water allowed to solubilize both the reagents and the halide salts stoichiometrically produced during the process and leading to a homogeneous reaction mixture that can be processed in flow. Finally, we have also completed the protocol by combining a downstream in-line liquid/liquid continuous separation that allowed to efficiently recover and reuse the CPME fraction facilitating the work-up and minimizing the waste-generation.

Results and discussion

Our investigation began with the design and the preparation of an hybrid organic-inorganic support for supporting palladium nanoparticles (Pd NPS). Silica SIPERNAT 320 (Evonik) was employed as inorganic support, having a moderate absorption capacity and BET specific surface area (SSA) of 164 m^2/g.

Former works showed that Si-Gly-Und-CD support proved efficient and homogeneous impregnation of small Pd NPs exhibiting excellent activity.[14g] It was demonstrated an amino alcoholic spacer and β-CD derivative effectively immobilize and stabilize PdNPs thanks to chelating and inclusive properties making both groups elemental for Pd anchoring. Its preparation started derivatizing silica with 3-glycidoxypropyltrimethoxysilane (GPMS), which was then reacted with 10-undecynil-1-amine (Und) to obtain an alkyl hydroxyl amino spacer prior β-CD anchor through a Cu-catalyzed azide–alkyne cycloaddition with 6^I-monoazido-6^I-deoxy-β-CD (Scheme 2).[22]

Aiming at simplifying the already established system (Si-Gly-Und-CD) in terms of synthetic steps, two different hybrid supports were also designed: Si-Gly derivative was grafted with 6^I-amino-6^I-deoxy-β-CD which opened the epoxide ring reducing the length of the hydroxyl amino spacer (Si-Gly-CD), afterwards a third support was achieved consisting of β-CD directly bound to silica previously converted to silica chloride using thionyl chloride, followed by nucleophilic substitution with 6^I amino-6^I-deoxy-β-CD (Si-NH-CD) (Scheme 2).

As reported in previous works, [14e] the beneficial effect of ultrasound (US) irradiation was exploited to maximize the grafting of GPMS and the synergic effect of combined MW and US irradiation were used when Si-Gly derivative was reacted with 6^I-amino-6^I-deoxy-β-CD[22] achieving an efficient grafting of β-CD in 4h at 100°C. The reaction in absence of enabling technologies requested 16 hrs to reach same results.

Synthetized silica derivatives were characterized by infrared spectroscopy (IR) and the grafting efficacy was measured from the percentage weight loss by thermogravimetric analysis (TGA) performed in the selected temperature range from 150°C to 800°C to discard the influence of solvents in the yield measure.

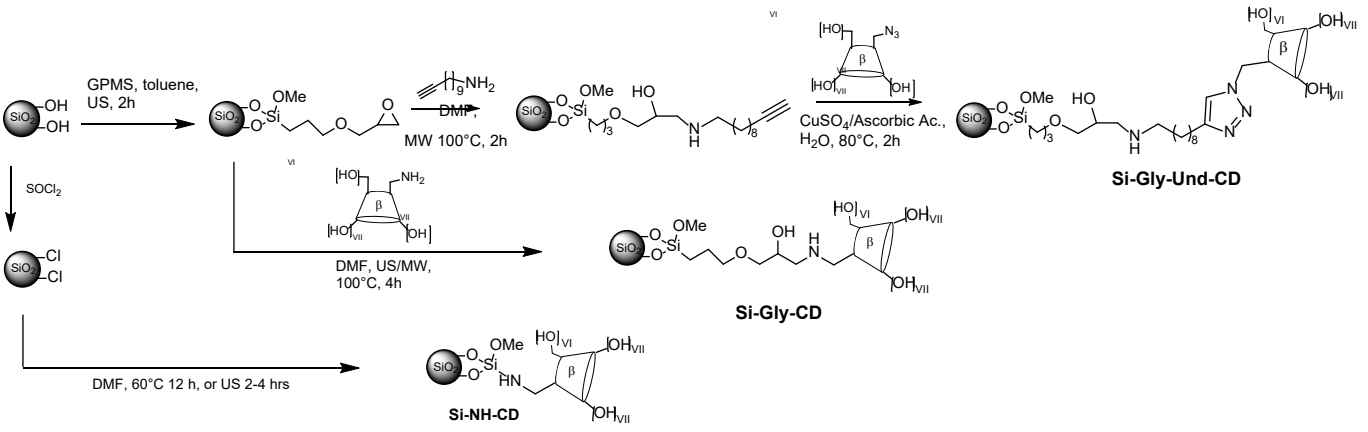

Scheme 2. Synthetic routes to solid supported CDs (Si.Gly-Und-CD; Si-Gly; Si-NH-CD.

Different batches of directly grafted Si-NH-CD were prepared and despite the fact that the Si-Cl intermediate was always titrated before the reaction with β-CD we observed a limit in reproducibility. TGA analysis showed a constant decomposition of the sample therefore we could not evidence any degradation step. Differently, as showed in Figure 1, the first derivative peak

temperature of Si-Gly-Und-CD was detected at 309°C while the second was at 549°C and a comparable trend was evidenced for Si-Gly-CD that starts the first thermal degradation at 319 °C while a second was detected at 489 °C. Results collected from different preparation of Si-Gly-Und-CD and Si-Gly-CD demonstrated a good reproducibility of grafting efficiency. As described in table 1 the efficiency of grafting was measured on the basis of weight loss by TGA by comparison of different synthetic steps. The amount of loaded β-CD measured was from 57 to 130 µmol/g in the three derivatives.

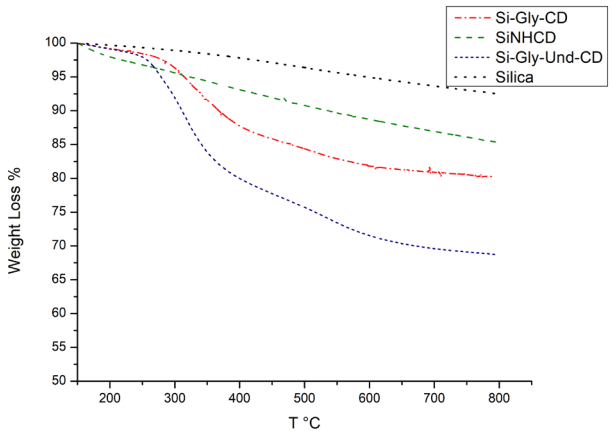

Figure 1. TGA profiles of organic inorganic silica derivatives: (a) Silica; (b) Si-Gly; (c) Si-Gly-CD.

The quantification of grafted β-CD with unchanged inclusive properties was evaluated by loss of UV absorbance at 553 nm of phenolphthalein (Php) when included in the β-CD cavity after treatment of a Php water solution with a weighted amount of β-CD-silica.[14f] The high specificity of this titration highlights only the CDs available for the formation of the complex and we could observe differences when a spacer is used to maintain inclusive capacity of cyclodextrin, therefore Si-Gly-Und-CD showed with the titration with PhP a comparable loading with respect to the TGA.

Table 1. Loading quantification of grafted silica derivatives.

Support	Loading % w/w	Loading µmol/g
Si-Gly	6.373[a]	275[a]
Si-Gly-CD	6.39[b]–1.94[c]	57[b] –17 [c]
Si-Gly-Und-CD	17.2[b]- 9.3[c]	130[b]-83[c]
Si-NH-CD	6.9[b]-0.75[c]	70[b]-7 [c]

[a] Gly amount measured by TGA, [b] β-CD grafting measured by TGA, [c] β-CD grafting measured by PhP titration

The infrared spectrum of hybrid Si-βCD supports (see supporting info) shows the fingerprint modes of CD between 1500 and 1250 cm^{-1} (δCH and δOH bending modes). The intense CH/CH_2 stretching modes (νCH/CH2) at 2928 and 2856 cm^{-1} prove the presence of alkylic chain in Si-Gly-CD and in Si-Gly-Und CD. The broad absorption between 3000 and 3750 cm^{-1} is related -OH groups from the CD rings and Si-OH groups fromthe silica surface (See ESI). νNH band at 1660 cm-1 can be seen and the IR spectrum of Si-Gly-Und-CD showed also a band at 1630 with a shoulder that correspond to the triazolyl group ring vibrations.

PdNPs were immobilized on the supports by reduction of the $Pd(OAc)_2$ precursor in ethanol with heating at reflux.

As already reported for the prepration of the Pd NPs supported on Si-Gly-Und-CD, the XRD patterns of the catalysts show that PdNPs exist on the Pd/Si-CD substrates (Figure 2). As represented in Figure 2, typical diffused scattering of the amorphous SiO_2 support gave the strongest peak in the XRD pattern (21.868). The other peaks are indexed as the (111), (2 0 0), (2 2 0), and (3 11) planes of the PdNPs (cubic phase, JCPDS 46-1043). With respect to standard references, a slight shift in the 2θ values is observed, for all peaks, and we can assume that a small increase in crystallite θ spacing happens as a consequence of particle nanosize.

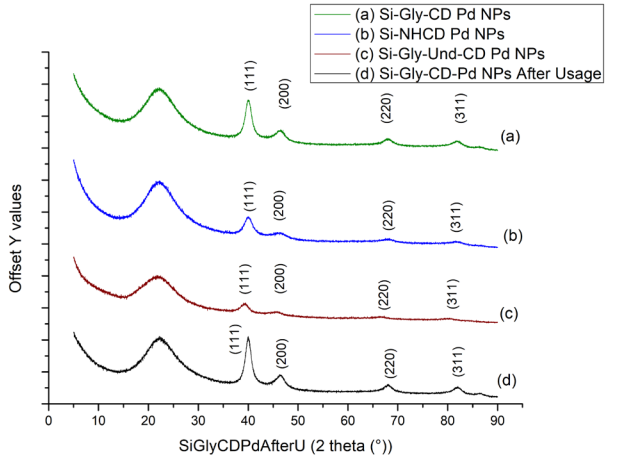

Figure 2 XRD patterns measured on samples listed in Table 1: a) Si-Gly-CD-PdNPs; b) Si-CD -PdNPs; c) Si-Gly-Und-CD-PdNPs and d) SiGlyCD-PdNPs After Usage.

From the Inductively coupled plasma (ICP) analyses carried out on the catalysts, palladium loading data were afforded (Table 2). Results showed that all the Si-CD supports load efficiently Pd NPs.

Table 2. . PdNPs loading (% w/w) from ICP analysis.

Catalyst	Loading % w/w
Si-Gly-Und-CD-PdNPs	2
Si-Gly-CD-PdNPs	1.8
Si-CD-PdNPs	2.2

All three catalysts were preliminary tested in a C-C Heck coupling reaction to evaluate if comparable catalytic activities could be observed. As previously optimized, styrene may efficiently react with iodo-benzene in presence of 0.5 mol% of Pd(NPs) supported on Si-Gly-Und-CD at 120 °C in MW for 1h.[14g] The reaction gave successfully >99% on conversion with both Si-Gly-Und and Si-Gly-CD supported Pd nanocatalyst. 82% conversion was observed with Si-NH-CD (see ESI). Although it enables comparable Pd adsorption this support showed limit in preparation reproducibility and lower synthetic activity

therefore it was discarded. Since the **Si-Gly-CD-PdNPs** showed comparable reactivity, stability, a reliable and simplified synthesis when compared to the Si-Gly-Und derivative, it was selected for tests carried out in this work. Surprisingly we observed that the inclusive capacity of CD does not affect the loading capacity of the PdNPs and its catalytic activity.

TEM images of the catalysts Si-Gly-CD-PdNPs are shown in Figure 3. Solid supported catalyst consists of uniform (mainly spheroidal) particles with a diameter range 2– 8 mm (Figure 3, particle distribution). Surprisingly by comparison with the Si-Gly-Und CD Pd NPs already studied, we could observe that Pd smaller particles supported on Si-Gly-CD were present with a comparable uniformity of istribution. We could also conclude that TEM and XRD data were in accordance.

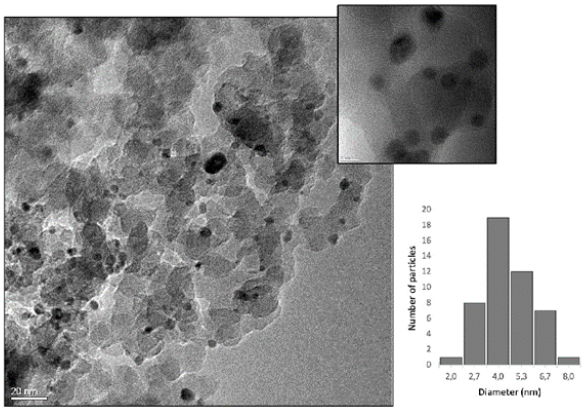

Figure 3. TEM images of Si-Gly_CD Pd NPs. Pd particle size distribution is also reported.

With the catalyst in hand, we started to test the catalytic performance in the model Sonogashira coupling between iodobenzene **1a** and phenylacetylene **2a** in presence of DABCO as a base. We screened environmentally friendly reaction media, different common petrol-based solvents, and their combination with water for the preliminary selection of the best reaction conditions (Table 3).

The catalyst showed good performance in almost all the reaction media tested. Interesting is the enhanced catalytic activity when a mixture of solvent/water was employed. This behaviour is attributable to the hybrid nature of our **Si-Gly-CD-PdNPs** catalyst. Indeed, the presence of β-CDs make the hybrid heterogeneous system water-friendly. It is worth to note that the benefits achieved from the presence of water are strictly related to its ratio with organic solvent (see for example Table 3 entries 1-3).

Moreover, when the organic solvent and water forms an azeotropic mixture, homogeneous or heterogeneous, the improvement in catalytic activity is remarkable. When pure CH_3CN is used as solvent 70% of product **3a** was obtained (Table 3, entry 6) while, in CH_3CN/water azeotropic mixture the conversion increased up to 85% (Table 3, entry 7). The same increment was observed also for CPME (Table 3, entry 13) and CPME/water heterogeneous azeotrope (Table 3, entry 14) leading to a 97% of conversion in product **3a** with high isolated yield.

With the optimized reaction conditions, we proceeded to test the stability and durability of our catalyst in the selected reaction medium CPME/water azeotrope.

Table 3. Screening of reaction media for Sonogashira cross-coupling of **1a**.[a]

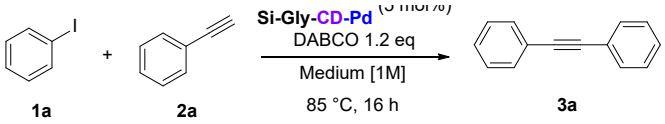

1a **2a** **3a**

entry	Medium	C [%][b]
1	DMF	90
2	DMF/water (6:1)	92
3	DMF/water (2:1)	88
4	NMP	70
5	NMP/water (2:1)	73
6	CH_3CN	70
7	CH_3CN/water az.	85
8	Propylene carbonate	87
9	Ethylene carbonate	89
10	GVL	90
11	GVL/water (2:1)	92
12	2-Me-THF	87
13	CPME	85
14	CPME/water az.	97 (94)[c]
15	Water	74
16	Water+SDS	88

[a] Reaction conditions: **1a** (1 mmol), **2a** (1.5 mmol), base (1.2 eq), Si-Gly-CD-PdNPs (5 mol%), solvent (1 mL, 1M), 85°C, 16h. [b] GLC conversion has been determined using samples of pure compound as reference standards; the remaining materials are **1a** and **2a**. [c] Isolated yield is given in parenthesis.

Table 4. Catalyst recycling and reuse in batch conditions[a]

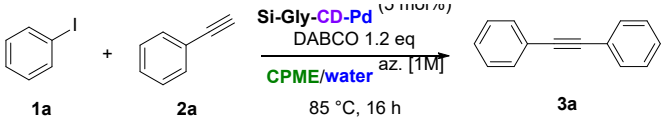

1a **2a** **3a**

Run	C [%][b]	Leaching (%)[c]
1	97 (94)	0.94
2	97 (94)	0.86
3	97 (94)	0.86

[a] Reaction conditions: **1a** (1 mmol), **2a** (1.5 mmol), DABCO (1.2 eq),), Si-Gly-CD-PdNPs (5 mol%), CPME/water az (1 mL, 1M), 85°C, 16h. [b] GLC conversion has been determined using samples of pure compound as reference standards; the remaining materials are **1a** and **2a.** [c] Determined with MP-AES, as percentage from the initial content of the fresh catalyst.

As expected, the catalyst showed very promising results in terms of recyclability allowing to be reused for three representative consecutive runs without loss in catalytic efficiency. Moreover, the catalyst was further stressed by performing recycling experiments at half conversion (Figure 4) showing a good durability.[21]

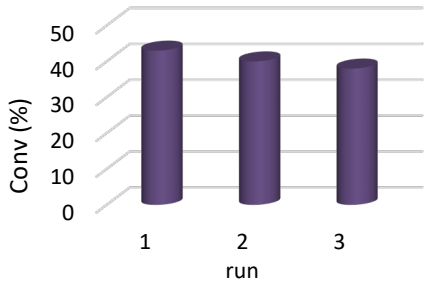

Figure 4. Catalyst recycles at $t_{1/2}$ in batch conditions. Reaction conditions: **1a** (1 mmol), **2a** (1.5 mmol), catalyst (5 mol%), DABCO (1.2 eq), solvent (1 mL, 1M), 7 h.

With these promising results under batch conditions, we began to plan the assembly of our flow system. We packed the Si-Gly-CD-PdNPs catalyst inside a stainless-steel reactor and we installed it into a thermostated box. The system has been designed by using two channels for the delivery of the reactant through the catalyst column (Figure 5).

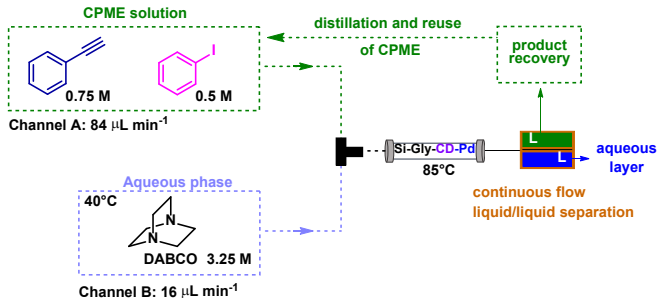

Figure 5. Continuous Flow system for the Sonogashira Reaction.

The channel A was charged with a CPME solution of **1a** and **2a** (0.5M and 0.75M respectively) while the channel B with a 3.25 M aqueous solution of DABCO and kept at 40 °C. The flow rates of the two channels have been regulated in order to have the exact azeotropic ratio of CPME/water inside the reactor (see ESI for further details).

Further optimizations of the other flow parameters were conducted to achieve a stable and durable conversion over the time (Table 5). When 100-250 BPRs were used, poor conversion was obtained associated with a low residence time (Table 5, entries 3-4). While, increasing the residence time to 35-50 minutes from good to excellent conversions into product **3a** were recorded (Table 5, entries 4-7).

At the output of the reactor, a liquid/liquid membrane separator was installed for the separation of the reaction mixture in the two pure components. These features allow us to also optimize the work-up procedure. Indeed, by evaporation and recovery of the CPME we were also able to reuse it continuously, while the aqueous DABCO-I solution represents the sole waste of the reaction.

Table 5. Optimization of flow parameters

entry	Channel A (mL/min)	Channel B (mL/min)	BPR (psi)	Residence time	C [%][a]
1	0.840	0.160	500	10 min	9
2	0.420	0.080	500	20 min	48
3	0.420	0.080	250	7 min	3
4	0.420	0.080	100	5 min	3
5	0.168	0.032	500	35 min	60
6	0.084	0.016	500	50 min	99
7	0.084	0.016	250	40 min	93

[a] GLC conversion has been determined using samples of pure compound as reference standards; the remaining materials are **1a** and **2a**.

With the optimized continuous-flow set-up we started to explore the scope of the Sonogashira reaction achieving high yields for all the substrates screened (Scheme 3).

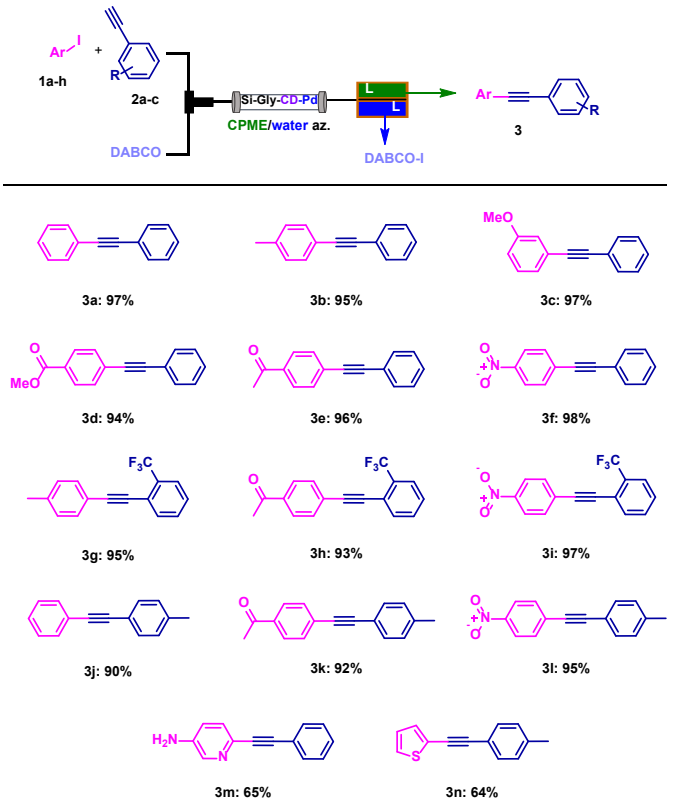

Scheme 3. Scope of Sonogashira in flow. Isolated yields are reported.

Both electron withdrawing and electron donating group on the iodoarene are well tolerated as well as electron donating group in the acetylenic compound leading to excellent isolated yields (90-98 %). Moreover, our continuous flow set-up showed good

performance also when iodo-heterocycles (**1g-h**) were coupled with phenylacetylene **2a** and deactivated alkyne **2c**.

By employing the designed flow set-up, we were able to efficiently convert 20 mmol of the differently substituted iodo-arene, heterocycles and phenylacetylenes with only 0.06 mmol of palladium (350 mg of Si-Gly-CD-PdNPs catalyst) proving the catalyst stability and durability. In these conditions, and after 10 h of continuous operation, the catalyst showed a TON value of 333 and a TOF of 33 h^{-1}.

In addition, the palladium leaching was periodically monitored during the flow operation (Figure 6). The value recorded are extremely low in the first 5 h of flow procedure with an additional reduction over the next hours. The TEM images of Si-Gly-CD-PdNPs (see supporting information) showed that Pd NPs lost uniformity in dispersion because nanoparticles agglomerate after usage. Looking at XRD analysis of catalyst after usage sharper peaks were observed to demonstrate an inclese in average crystallite size.

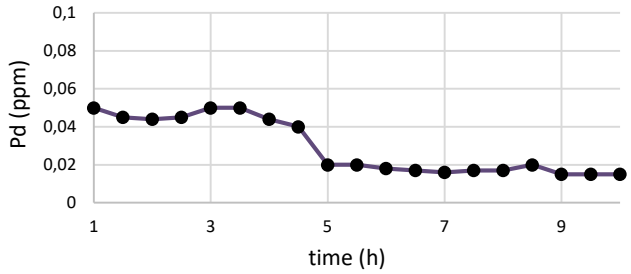

Figure 6. Leaching of metal in solution

In order to evaluate the efficiency of the catalyst utilized in the newly developed flow reactor, we have also tested more challenging aryl-bromide as substrates. Under identical conditions in flow aryl-bromide **4a** and **4b** gave high isolated yield of the corresponding coupling products. We therefore also finalized our study in the the synthesis of API intermediates **3o** and **3p** obtained by coupling 6-Br-nicotinaldehyde **4c** and 6-Br-nicotinic acid **4d** with trimethylsilylacetylene **2d** (Scheme 4).

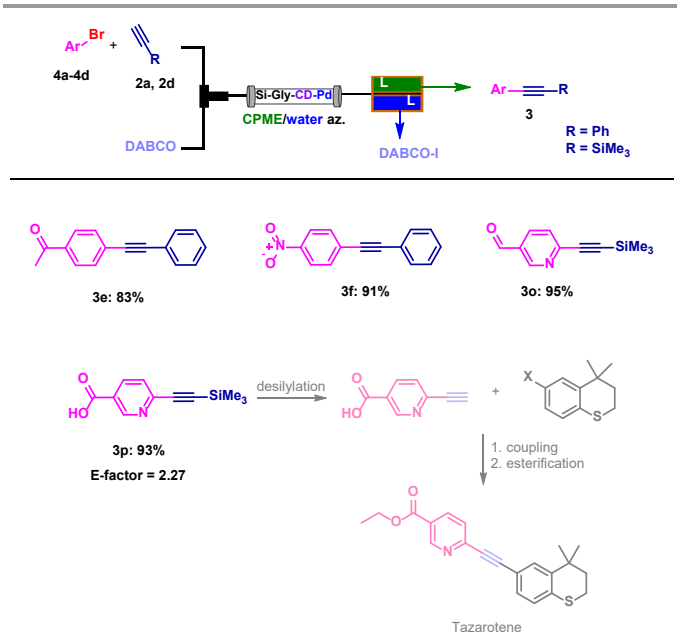

Scheme 4. Scope of Sonogashira in flow using aryl-bromide. Isolated yields are reported.

Compound **3p** is obtained with an E-factor of 2.27, and it is the key intermediate that by already reported procedures,[23] after desilylation and coupling with 6-halo-4,4-dimethylthiochromane allows to prepare obtain the API Tazarotene. Finally, in order to evaluate the sustainability improvement of our protocol, we focused the attention into a comprehensive and general assessment of the environmental features. Initially we calculated the mass-dependent metrics (E-factor) for the whole procedure and for other representative similar flow processes (Figure 7. Due to the CPME recovery and reuse, the E-factor value associated with our flow set-up is extremely low (2.12).

Aiming at the identification of the major contributions to the very low E-factor values,[24] we observed that the mixture concentration and the auxiliary material strongly affected the waste production (See Supporting Info for further details).

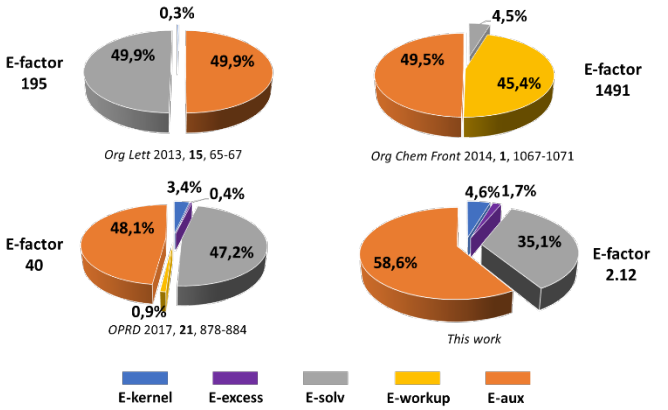

Figure 7. E-factor distribution analysis

In addition, to gain more insight, we analysed different green metrics in terms of Vector Magnitude Ratio by adopting the radial polygon analysis (Figure 8).[25]

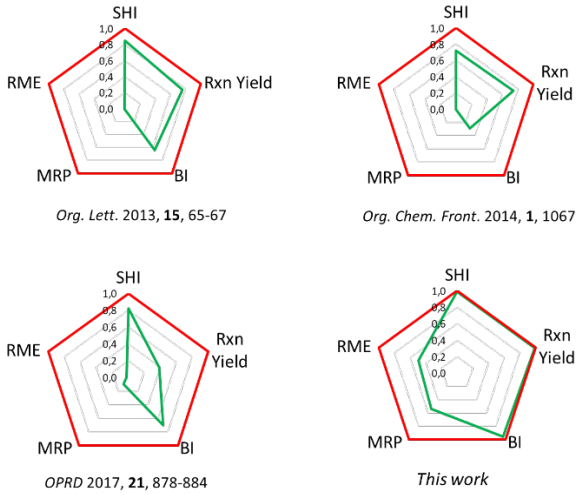

Figure 8. Environmental and safety analyses based on radial polygons.

In these analyses we also have included the determination of the Benign Index (BI) and the Safety Hazard Index (SHI) associated to the waste material.

This comparison highlights that the reclaim of the solvent mainly influenced the environmental profile exploited by our flow assisted Sonogashira reaction. In addition, the BI and SHI highly benefit from the use of CPME as environmentally friendly solvent and DABCO as base, which have higher Flash Point (62.2 °C) in comparison with triethylamine (-11 °C)[16a] and diisopropylethylamine (9. 5 °C),[16d] and low vapour pressure (72 hPa at 23 °C).

Conclusions

In conclusion, here we reported a flow-assisted Sonogashira cross-coupling reaction catalysed by Si-Gly-CD-PdNPs hybrid catalyst. The catalytic efficiency was improved by exploiting the hydrophilicity of the β-CD ligand allowing the utilization of a CPME/water azeotropic mixture. The selected reaction medium and flow technology led to a dramatic minimization of metal leaching in solution, improving catalyst stability and durability.

Moreover, the synergy between the recovery of CPME and the packed-bed flow technology, allow us to achieve great improvement in terms of waste reduction. The designed methodology allowed the continuous flow production of 20 mmol of differently substituted compound with only 0.06 mmol of palladium.

The environmental features were also evaluated based on the green-metrics and by considering the safety hazard and the benign index associated to the waste material.

Acknowledgements

The Università degli Studi di Perugia and MIUR are acknowledged for financial support to the project AMIS, through the program “Dipartimenti di Eccellenza - 2018-2022”. The University of Turin is acknowledged for the financial support (ricerca locale 2020). We thank M. C. Valsania (Mayita) from the Microscopy Laboratory of the NIS Centre and Prof G. Berlier for their precious help.

Notes and references

1 a) H. A. Dieck, F. R. Heck, *Journal of Organometallic Chemistry*, 1975, **93**, 259-263; b) L. Cassar, *Journal of Organometallic Chemistry,* 1975, **93**, 253-257; c)K. Sonogashira, Y. Tohda, N. Hagihara, Tetrahedron Lett. 1975, **50**, 4467-4470.

2 a) R. Chinchilla, C. Nájera, *Chem. Rev.* 2014, **114**, 1783−1826; b) R. Chinchilla, C. Nájera, *Chem. Soc. Rev*. 2011, **40**, 5084–5121; c) C. Torborg, M. Beller *Adv. Synth. Catal*. 2009, **351**, 3027–3043; d) R. Chinchilla, C. Nájera, *Chem. Rev.* 2007, **107**, 874–922.

3 a) I. Favier, D. Pla, M. Gomez, *Chem. Rev*. 2020, **120**, 1146–1183; b) A. Biffis, P. Centomo, A. Del Zotto, M. Zecca, *Chem. Rev.* 2018, **118**, 2249–2295; c) A. Molnar, *Chem. Rev*. 2011, **111**, 2251–2320; d) I. J. S. Fairlamb, N. W. J. Scott, 2020, Pd Nanoparticles in C–H Activation and Cross-coupling Catalysis in Nanoparticles in Catalysis, 2020, 171-205

4 a) A. Bavykina, N. Kolobov, I. S. Khan, J. A. Bau, A. Ramirez, J. Gascon, *Chem. Rev*. 2020, **120**, 8468–8535; b) D. Sciosci, F. Valentini, F. Ferlin, S. Chen, Y. Gu, O. Piermatti and L. Vaccaro, *Green Chem*., 2020, **22**, 6560–6566; c) S. Mujahed, F. Valentini, S. Cohen, L. Vaccaro and D. Gelman, *ChemSusChem*, 2019, **12**, 4693–4699 d) F. Valentini, G. Brufani, L. Latterini, L. Vaccaro, Metal Nanoparticles Catalyzed C–C Bond Formation via C–H Activation in Advanced Heterogeneous Catalysts Volume 1: Applications at the Nano-Scale, 2020, 513-543.

5 a) E. Heuson, R. Froidevaux, I. I. Jr, R. Wojcieszak, M. Capron, F. Dumeignil, *Green Chem*., 2021, Advance Article; b) M. Kalaj, K. C. Bentz, S. Ayala Jr., J. M. Palomba, K. S. Barcus, Y. Katayama, S. M. Cohen, *Chem. Rev*. 2020, **120**, 8267–8302; c) M. Liras, M. Barawi, V. A. de la Pena O’Shea, *Chem. Soc. Rev*., 2019,**48**, 5454-5487; d) U. Diaz, D. Brunel, A. Corma, *Chem. Soc. Rev.,* 2013, **42**, 4083-4097.

6 a) E. D. Goodman, C. Zhou, M. Cargnello, *ACS Cent. Sci*. 2020, **6**, 1916−1937; b) Y. Wang, L. Chen, C.-C. Hou, Y.-S. Wei, Q. Xu, *Org. Biomol. Chem*., 2020, **18**, 8508-8525; c) Y. Ding, P. Zhang, H. Xiong, X. Sun, A. Klyushin, B. Zhang, Z. Liu, J. Zhang, H. Zhu, Z.-A. Qiao, S. Heumann, S. Dai, *Green Chem*., 2020, **22**, 6025-6032; d) R. Ye, J. Zhao, B. B. Wickemeyer, F. D. Toste, G. A. Somorjai, *Nature Catalysis*, 2018, **1**, 318-325.

7 B. Lei, B. Li, H. Zhang, L. Zhang, W. Li, *J. Phys. Chem. C* 2007, **111**, 11291-11301.

8 M. Benzaqui, R. Semino, F. Carn, S. R. Tavares, N. Menguy; M. Giménez-Marqués; E. Bellido, P. Horcajada, T. Berthelot; A. I. Kuzminova; M. E. Dmitrenko, V. A. Penkova, D. Roizard, C. Serre, G. Maurin, N. Steunou, *ACS Sustain. Chem. Eng*. 2019, **7**, 6629–6639.

9 a) N. Lashgari, A. Badiei, G. Mohammadi Ziarani, *Nanochem. Res.* 2016, **1**, 127–141; b). S. Singh, R. Kumar, H. D. Setiabudi, S. Nanda, D.-V. N. Vo, *Appl. Catal. A Gen*. 2018, **559**, 57–74; c) M. J. Ndolomingo, R. Meijboom,. *Catal. Lett*. 2019, **149**, 2807–2822; d) D. Chen, P. Zhang, Q. Fang, S. Wan, H. Li, S. Yang, C. Huang, S. Dai, *Inorg. Chem. Front*. 2018, **5**, 2018–2022.

10 a) A. Azeez, L. Polio, J. E. Hanson, S. M. Gorun, *ACS Appl. Polym. Mater*. 2019, **1**, 1514–1523; b) P. P. Fedorov, A. A. Luginina, S. V. Kuznetsov, V. V. Voronov, A. A. Lyapin, P. A. Ryabochkina, M. V. Chernov, M. N. Mayakova, D. V.

Pominova, O. V. Uvarov, A. E. Baranchikov, V. K. Ivanov A. A. Pynenkov, K. N. Nishchev *J. Fluor. Chem.* 2017, **202**, 9–18.

11 a) N. Ahadi, M. A. Bodaghifard, A. Mobinikhaledi, *Appl. Organomet. Chem.* 2019, **33**, e4738; b) M. Fallahi, E. Ahmadi, Z. E. Mohamadnia, *Appl. Organomet. Chem.* 2019, **33**, e4975.

12 a) W. Li, Y. Zhang, Q. Li, G. Zhang, *Chem. Eng. Sci.* 2015, **135**, 232–257; b) P. T. Yin, S. Shah, M. Chhowalla, K.-B. Lee, *Chem. Rev.* 2015, **115**, 2483–2531.

13 T. Skorjanc, F. Benyettou, J. C. Olsen, A. Trabolsi, *Chemistry* 2017, **23**, 8333–8347.

14 a) M. I. Velasco, C. R. Krapacher, R. H. de Rossi, L. I. Rossi, *Dalton Trans*. 2016, **45**, 10696–10707; b) G. Kurokawa,M. Sekii, T. Ishida, T. Nogami, *Supramol. Chem.* 2004, **16**, 381–384; c) L. I. Rossi, C. O. Kinen, R. H. de Rossi, R.H. *Comptes Rendus Chim.* 2017, **20**, 1053–1061; d) F. Calsolaro, K. Martina, E. Borfecchia, F. Chavez-Rivas, G. Cravotto, G. Berlier, *Catalyst,* 2020, **10**, 1118; e) K. Martina, F. Calsolaro, A. Zuliani, G. Berlier, F. Chavez-Rivas, M. J. Moran, R. Luque, G. Cravotto, *Molecules*, 2019, **24,** 2490; f) E. C. Gaudino, S. Tagliapietra, G. Palmisano, K. Martina, D. Carnaroglio, G. Cravotto, *ACS Sustainable Chem. Eng.* 2017, **5**, 9233–9243; g) K. Martina, F. Baricco, M. Caporaso, G. Berlier, G. Cravotto, *ChemCatChem*, 2015, **8**, 1176-1184; h) K. Martina, F. Baricco, G. Berlier, M. Caporasso, G. Cravotto, *ACS Sustainable Chem. Eng*. 2014, **2**, 2595–2603; i) Han, B.-H.; Antonietti, M. *J. Mater. Chem.* 2003, **13**, 1793–1796; l) S. Bahadorikhalili, L. Ma'mani, H. Mahdavi, A. Shafiee, *Microporous Mesoporous Mater*. 2018, **262**, 207–216; m) R.-P. Ye, L. Lin, C.-Q. Liu, C.-C. Chen, Y.-G. Yao, *ChemCatChem* 2017, **9**, 4587–4597; n) A. A. Fedorova, I. V. Morozov, Y. N. Kotovshchikov, B. V. Romanovsky, S. V. Sirotin, E. E. Knyazeva, A. S. Lermontov, A. S. Shaporev, *Mendeleev Commun*. 2011, **21**, 171–172.

15 a) M. Cortes-Clerget, J. Yu, J. R. A. Kincaid, P. Walde, F. Gallou, B. H. Lipshutz, *Chem. Sci*., 2021, Advance Article doi.org/10.1039/D0SC06000C; b) F. Mohajer, M. M. Heravi, V. Zadsirjan, N. Poormohammad, *RSC Adv*., 2021, **11**, 6885-6925; c) Y. Baqui, *Catalysts* 2021, **11**, doi.org/10.3390/catal11010046; d) L. Zhou, S. Li, B. Xu, D. Ji, L. Wu, Y. Liu, Z.-M. Zhang, J. Zhang, *Angew.Chem. Int.Ed*. 2020, **59**, 2769 –2775; f) B. Feng, Y. Yang, J. You, *Chem. Commun.,* 2020, **56**, 790-793; g) A. S. Díaz-Marta, S. Yañez, E. Lasorsa, P. Pacheco, C. R. Tubío, J. Rivas, Y. Piñeiro, M. A. Gonzalez Gómez, M. Amorín, F. Guitián, A. Coelho, *ChemCatChem* 2020, **12**, 1762 – 1771; h) Y. Tian, J. Wang, X. Cheng, K. Liu, T. Wu, X. Qiu, Z. Kuang, Z. Li, J. Bian, *Green Chem*., 2020, **22**, 1338-1344; i) D.-L. Zhu, R. Xu, Q. Wu, H.-Y. Li, J.-P. Lang, H.-X. Li, *J. Org. Chem*. 2020, **85**, 9201–9212.

16 a) D. Znidar, C. A. Hone, P. Inglesby, A. Boyd, C. O. Kappe, *Org. Process Res. Dev.* 2017, **21**, 878–884; b) I. Penafiel, A. Martinez-Lombardia, C. Godard, C. Claver A. Lapkin, *Sustainable Chemistry and Pharmacy*, 2018, **9**, 69–75; c) S. Voltrova, J. Srogl, *Org. Chem. Front*., 2014, **1**, 1067-1071; d) L.-M. Tan, Z.-Y. Sem, W.-Y. Chong, X. Liu, Hendra, W. L. Kwan, C.-L. Ken Lee, *Org. Lett.* 2013, **15**, 65–67.

17 a) M. A. Newton, D. Ferri, C. J. Mulligan, I. Alxneit, H. Emerich, P. B. J. Thompson, K. K. Hii, *Catal. Sci. Technol*., 2020, **10**, 466-474; b) F. Ferlin, P. M. Luque Navarro, Y. Gu, D. Lanari, L. Vaccaro, *Green Chem*., 2020, **22**, 397-403; c) F. Ferlin, M. K. Van der Hulst, S. Santoro, D. Lanari, L. Vaccaro, *Green Chem*., 2019, **21**, 5298-5305; d) F. Ferlin, T. Giannoni, A. Zuliani, O. Piermatti, R. Luque, L. Vaccaro, *ChemSusChem* 2019, **12**,3178 –3184; e) F. Ferlin, M. Cappelletti, R. Vivani, M. Pica, O. Piermatti, L. Vaccaro, *Green Chem*., 2019, **21**, 614-626; f) E. M. Barreiro, Z. Hao, L. A. Adrio, J. R. van Ommen, K. Hellgardt, K. K. Hii, *Catalysis Today*, 2018, **308**, 64–70; g) L. Vaccaro, M. Curini, F. Ferlin, D. Lanari, A. Marrocchi, O. Piermatti, V. Trombettoni, 2018, **90**, 21-33; h) J. B. Brazier, B. N. Nguyen, L. A. Adrio, E. M. Barreiro, W. P. Leong, M. A. Newton, S. j. A. Figueroa, K. Hellgardt, K. K. Hii, *Catalysis Today*, 2014, **229**, 95–103.

18 a) Y. Mohr, M. Alves-Favaro, R. Rajapaksha, G. Hisler, A. Ranscht, P. Samanta, C. Lorentz, M. Duguet, C. Mellot-Draznieks, E. A. Quadrelli, F. M. Wisser, J. Canivet *ACS Catal*. 2021, **11**, 3507–3515; b) S. Checchia, C. J. Mulligan, H. Emerich, I. Alxneit, F. Krumeich, M. Di Michiel, P. B. J. Thompson, K. K. Hii, D. Ferri, M. A. Newton, *ACS Catal.* 2020, **10**, 3933–3944; c) F. Ferlin, S. R Yetra, S. Warratz, L. Vaccaro, L. Ackermann, *Chem. Eur. J.* 2019, **25**, 11427–11431; d) F. Ferlin, L. Luciani, O. Viteritti, F. Brunori, O. Piermatti, S. Santoro, L. Vaccaro, *Front. Chem*., 2019, **6**, 659.

19 F. Valentini, H.Mahmoudi, L. A. Bivona, O. Piermatti, M. Bagherzadeh, L. Fusaro, C. Aprile, A. Marrocchi, L. Vaccaro, *ACS Sustainable Chem. Eng*. 2019, **7**, 6939–6946; b) H. Mahmoudi, F. Valentini, F. Ferlin, L. A. Bivona, I. Anastasiou, L. Fusaro, C. Aprile, A. Marrocchi, L. Vaccaro, *Green Chem*., 2019, **21**, 355-360; c) F. Ferlin, L. Luciani, S. Santoro, A. Marrocchi, D. Lanari, A. Bechtoldt, L. Ackermann, L. Vaccaro, *Green Chem*., 2018, **20**, 2888-2893; d) E. Petricci, C. Risi, F. Ferlin, d. Lanari, L. Vaccaro, *Sci. Rep*. 2018, **8**, 10571; e) F. Ferlin, S. Santoro, L. Ackermann, L. Vaccaro, *Green Chem*., 2017, **19**, 2510-2514; f) G. Rubulotta, K. L. Luska, C. A. Urbina-Blanco, T. Eifert, R. Palkovits, E. A. Quadrelli, C. Thieuleux, W. Leitner, *ACS Sustainable Chem. Eng*. 2017, **5**, 3762–3767.

20 a) F. Valentini, L. Vaccaro, *Molecules* 2020, **25**, 5264; b) D. Rasina, A. Lombi, S. Santoro, F. Ferlin, L. Vaccaro, *Green Chem*. 2016, **18**, 6380–6386; c) F. Ferlin, V. Trombettoni, L. Luciani, S. Fusi, O. Piermatti, S. Santoro, L. Vaccaro, *Green Chem*. 2018, **20**, 1634–1639

21 U. I. Kramm, R. Marschall, M Rose, *ChemCatChem* 2019, **11**, 2563– 2574.

22 F. Trotta, K. Martina, B. Robaldo, A. Barge, G. Cravotto, *J. Incl. Phenom. Macrocycl. Chem*. 2007, **57**, 3–7

23 a) H. Xie, L. Ming, J. Wu, Y. Zhang, Y. Cheng, patent number: WO 2020/114494 A1 (2020); b) C. N. Jain, M. N. Vaghela, R. B. Rehani, R. Thenati, patent number: WO 2006/059345 A2 (2006); c) M. E. Garst, L. J. Dolby, N. A. Fedoruk, patent number: US005420295A (1995).

24 J. Andraos, *Green Process Synth*, 2019, **8**, 324–336, doi: 10.1515/gps-2018-0131

25 J. Andraos, *Org. Process. Res. Dev*. 2013, **17**, 175–192

